High-pH alteration of argillaceous rocks : an experimental study

High-pH alteration of argillaceous rocks: an experimental study

by *Michael Adler[1], Urs K. Mäder[1]* and *H. Niklaus Waber[1]*

Abstract

Diffusion and evaporatively-driven advection experiments were performed at 30 °C to investigate the effect of high-pH solutions on the mineralogy of whole rock Opalinus Clay. Reacted rock samples were analysed by SEM and XRD after 4, 6, 12 and 18 months in the diffusion experiments and after 7 and 12 months in the advection experiments. The sequence of reaction products under these high-pH conditions includes first the precipitation of zeolites and Ca-Al-Si-hydrate phases (C-A-S-H) followed by a clay mineral-calcite paragenesis which is accompanied by sulphates in the advection experiments. The formation of zeolites appears to be bound to closed-system reactions where conditions of low fluid fluxes accomplish a greater degree of local pH buffering of the solution thus providing suitable conditions for zeolite precipitation. Massive formation of calcite during later stages of rock-water interaction is attributed to dissolution of dolomite/ankerite which increases pCO_2 in solution and suppresses further precipitation of zeolites and C-A-S-H phases. The results of these investigations show that the mineralogy of Opalinus Clay is significantly changed by attack of high-pH solutions even at temperatures as low as 30 °C.

Keywords: waste disposal, advection experiments, high-pH solution, argillaceous rock, Opalinus Clay.

Introduction

Several designs for the geological disposal of low/intermediate-level radioactive wastes envisage the emplacement of the waste in cementitious repositories constructed in a stable host rock. Leaching of concrete and cement, which are proposed as waste matrix material, backfill material and structural components, by groundwater is known to produce high-pH conditions, which will significantly alter pore water composition, mineralogy, porosity and permeability of the surrounding rock. All these changes could effect radionuclide migration by altering the original retardation capacity of the host rock. The effect of high-pH solutions on different geological materials has been subject to numerous studies using a variety of different approaches, including natural analogue sites (SMELLIE et al., 1997; LINKLATER et al., 1996), reactive transport modeling (e.g. HAWORTH et al., 1987; STEEFEL and LICHTNER, 1994, 1998a, b) and laboratory experiments (e.g. BARTH-WIRSCHING and HÖLLER, 1989; BATEMAN et al., 1997, 1999; BAUER et al., 1998; CHERMAK, 1992, 1993, DIAMOND et al., 1964). The main objective of these studies has been to assess the stability of different rocks as barriers to the migration of aggressive alkaline solutions emanating from cementitious waste repositories.

Argillaceous rocks are under consideration as potential host rocks for low/intermediate-level and high-level radioactive waste repositories in several national programmes mainly due to their low permeabilities and high sorption capacities (BROOKINS, 1987).

The composition of high-pH pore fluids released during the breakdown of concrete has been modeled (REARDON, 1990; BERNER, 1990) and shows an early period of NaOH and KOH release with pH > 13 followed by solution compositions at portlandite ($Ca(OH)_2$) saturation (pH $\approx$ 12.5), and finally solutions controlled by the solubility of Ca-Si-hydrate (C-S-H) phases (pH between 9–10).

Experimental data on high-pH alteration of ground argillaceous material are available from batch experiments at elevated temperatures of 150–200 °C (CHERMAK, 1992, 1993) and from

[1] Rock-Water Interaction Group, Institute of Geology and Institute of Mineralogy and Petrology, University of Bern, Baltzerstrasse 1, CH-3012 Bern, Switzerland. <adler@mpi.unibe.ch.>

flow-through column experiments at 70 °C (BATE-MAN et al., 1999). The secondary minerals formed under these laboratory conditions include clay minerals, feldspars, zeolites and various C-S-H phases. However, the direct applicability of these results to a potential repository in Switzerland is questionable due to the high experimental temperatures compared to expected repository temperatures and because of the utilisation of ground rock, both of which aimed at speeding up mineral reactions to obtain results on a laboratory timescale (months to few years).

This present experimental investigation examines the effect of high-pH solutions on whole rock Opalinus Clay (middle Jurassic, Mont Terri, Northern Switzerland) samples at repository host rock relevant temperatures of 30 °C to provide a closer approach to the reality of a potential cementitious repository and aims at bridging the gap in evidence from powdered rock samples. The experiments are designed to investigate water-rock interaction in response to diffusive and advective transport of a fluid phase at conditions of high-pH.

Experimental Methods

Two types of experiments were performed with whole rock Opalinus Clay and K–Na–Ca–hydroxide solution, one ensuring closed-system behaviour, and the other mimicking open-system behaviour (Fig. 1). The fluid is a simplified version of an early alkali-rich leachate expected to emanate from a cementitious repository (Tab. 1). The mineral composition of Opalinus Clay is listed in table 2 and its water saturated porosity amounts to approximately 14 volume percent.

Special emphasis during sample preparation aimed at minimizing mechanical damage. A hand saw with a tungsten carbide studded wire blade allowed careful cutting of samples without inducing new fractures parallel to bedding. The samples were kept vacuum-sealed in plastic bags between all steps of sample preparation to preserve the in-situ moisture content. All surfaces of the samples were sealed with an epoxy resin by placing them into a piece of PVC drain pipe of appropriate diameter and then submersing completely in epoxy (Fig. 1). The PVC pipe additionally provided extra strength to prevent excessive fracturing of the sample parallel to the bedding during the experiments. The size of the rock samples was approximately 4 cm in diameter and 6 cm in length.

For the closed-system (or diffusion) experiments one rock surface was exposed by cutting the epoxy cylinder shortly before the beginning of

Tab. 1 Initial solute concentrations of high-pH fluid.

	Concentration [mol/l]
K$^+$	1.61×10^{-1}
Na$^+$	6.52×10^{-2}
Ca^{2+}	2.24×10^{-3}
T (°C)	25
pH	13.2

Tab. 2 Initial composition of Opalinus Clay.

Mineral	Weight %
kaolinite	25
illite	20
calcite	15
quartz	15
chlorite	10
mixed layer illite/smectite	10
K feldspar, albite, siderite, ankerite, dolomite, pyrite	5

the experiment. For the open-system experiments an additional surface was exposed to atmosphere (Fig. 1). All samples were arranged in such a manner that the exposed surfaces were oriented perpendicular to the bedding. The sample was then placed in a glass dish, whereby one open surface remained submerged in 150 ml high-pH solution. The second surface in the open-system experiments remained open to atmosphere in order to enhance fluid transport by evaporation and capillary forces. Evaporation from surfaces other than that of the exposed rock surface had to be prevented in order to relate weight loss measurements to fluid flux. This was accomplished by sealing the glass dish against the epoxy cylinder with a double layer of Parafilm® and adhesive tape. This construction also aimed at minimizing infiltration of atmospheric carbon dioxide.

Diffusion experiments were conducted under controlled N_2 atmospheric conditions whereas in the evaporatively-driven advection experiments, only the high-pH solution was isolated from air. All experiments were run in a ventilated drying oven at 30 °C. The solution in the glass dish was repeatedly agitated and the advection experiments were periodically weighed on a digital balance. The solution in each experiment was replaced every 3 to 4 months and the pH of replaced and new solutions were measured at 25 °C using a pH electrode.

Analyses on reacted rock samples were carried out after 4, 6, 12 and 18 months for the diffusion experiments and after 7 and 12 months for the advection experiments. Reaction products were characterized by scanning electron mi-
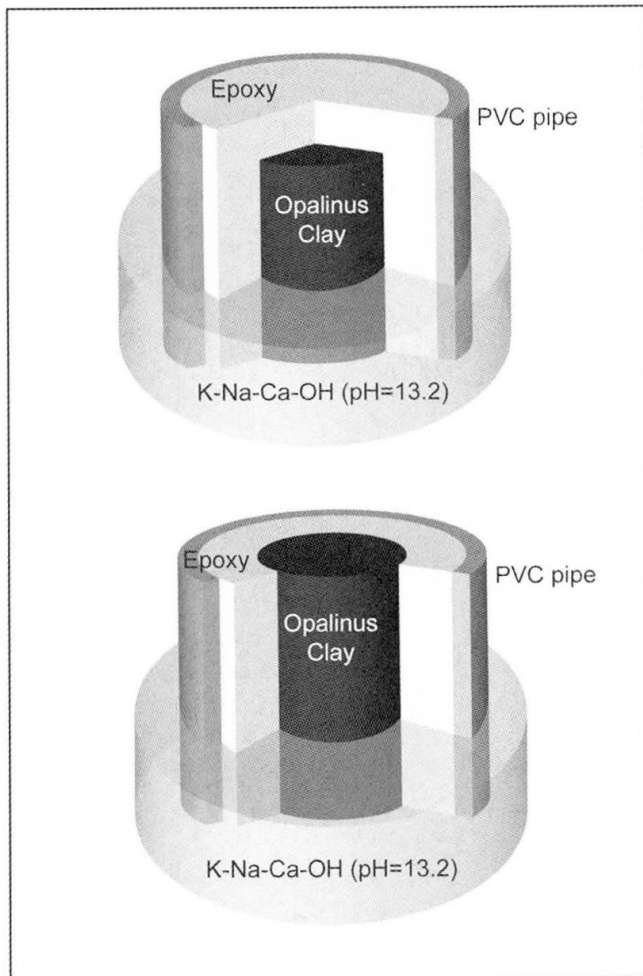
Fig. 1 Schematic of experimental setups. Top: diffusion experiments (closed system), bottom: evaporatively-driven advection experiments (open system). See text for details.

Results

DIFFUSION EXPERIMENTS

Measurements of reacted K–Na–Ca-hydroxide solutions show that pH decreased by one to three units after 3 to 4 months of reaction time with Opalinus Clay. Macroscopic observations on reacted Opalinus Clay samples showed rusty spots and stripes on the bottom surface of all samples due to pyrite oxidation and formation of Fe hydroxides. Macroscopically visible reaction fronts extending 0.5–1.0 μm into the rock matrix were observed after 6, 12 and 18 months, but not after 4 months. At 6 months, these zones are characterized by a rusty discoloration of the rock matrix whereas after 12 and 18 months, the matrix displays a leached, light gray color.

After 4 months, C-A-S-H gels formed on the infiltration surface of the samples (Fig. 2). The cauliflower-shaped gels have diameters of a few tenths of μm (Fig. 3a). After 6 months, neoformed (K-) Ca zeolites of mordenite-dachiardite composition with prismatic habit and lengths of 5 to 20 μm formed on bedding planes adjacent to the infiltration surface (Fig. 3b). The zeolites are partly overgrown by fibrous C-S-H phases with minor Al (Fig. 3c). A sparse calcite precipitation zone

croscopy (SEM) combined with energy dispersive spectrometry (EDS) and X-ray diffraction (XRD). For SEM analyses, rock pieces were mounted with a freshly fractured surface exposed on SEM holders and sputter-coated with gold. SEM and EDS analyses were used to characterize newly formed phases morphologically and chemically and to aid in confirming reaction products. XRD analyses (CuKα radiation) were carried out on the clay-size fraction (< 2 μm), as this was assumed to contain the largest amount of reaction products, and on isolated reaction products that were hand-picked under a binocular microscope. The isolation of reaction products was only applicable in few cases because of the small quantities of secondary phases, and XRD patterns of these were collected by measuring the material on silicon plates using long measurement durations.
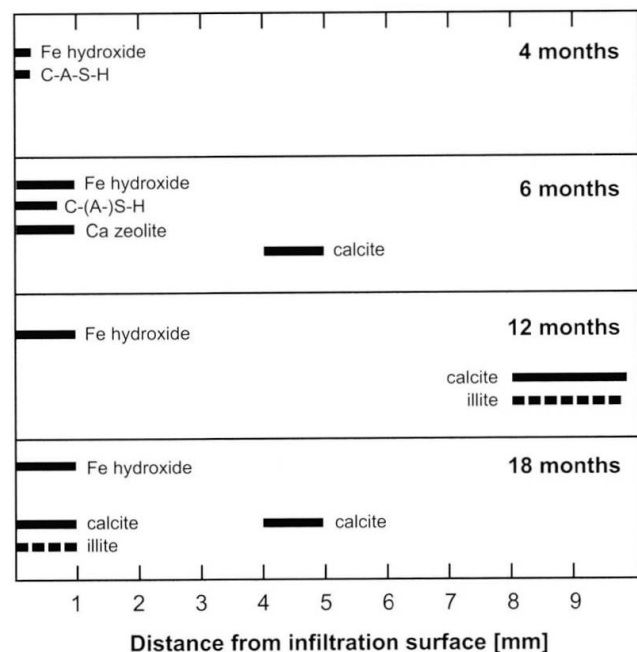

Fig. 2 Comparison of distribution of secondary minerals that formed in the diffusion experiments at different time steps. Only the first 10 mm above the infiltration surface are shown, above which no new phases were detected. Dashed bars indicate uncertain identification of a mineral phase. See text for details. C-A-S-H: Ca–Al–Si-hydrate phase.

was found further up the profile. The calcite crystals exhibit equant shapes and are a few μm in size. A massive calcite zone formed after 12 months ca. 1 cm above the infiltration surface, which is the maximum penetration depth of reaction products observed in the diffusion experiments. Two calcite precipitation zones developed after 18 months, a narrow zone adjacent to the infiltration surface (Fig. 3d) and a wider zone further up the profile. Grain-shapes in the lower zone are mainly equant, whereas the upper zone is composed of more irregularly shaped calcite. Zeolites and C-A-S-H phases are absent after 12 and 18 months. XRD bulk analyses on the clay fraction show a relative increase in illite content and a decrease in kaolinite contents compared with unaltered rock within some of the calcite zones in the 12 and 18 months experiments. However, the presence of newly formed illite could not be proven without ambiguity, neither by SEM nor by XRD.

All secondary minerals observed formed on bedding planes that functioned as preferential pathways for the high-pH solution.

ADVECTION EXPERIMENTS

Values of pH of reacted K–Na–Ca-hydroxide solutions decreased by one to two units after 3 to 4 months of reaction time. Periodic weight-loss measurements show that specific fluxes in both experimental runs steadily decrease and reach quasi steady states after approximately 140 days and remain constant at $3.3–4.0 * 10^{-6}$ kg sec^{-1} m^{-2} which, assuming a porosity of 14%, translates to two pore volumes per month.

Binocular microscopic observations on the samples which were reacted for 7 and 12 months show abundant patches of white reaction products along the whole length of the sample profile. They are up to 4 mm in diameter and made up of very fine-grained material which precipitated on clay mineral substrate as well as on calcitic shell debris. Moreover, partial oxidation of pyrite aggregates and formation of Fe hydroxides was observed along the whole length of the sample profile.

There is a chromatographic succession of different secondary mineral phases with increasing distance from the infiltration surface (Fig. 4). Gen-
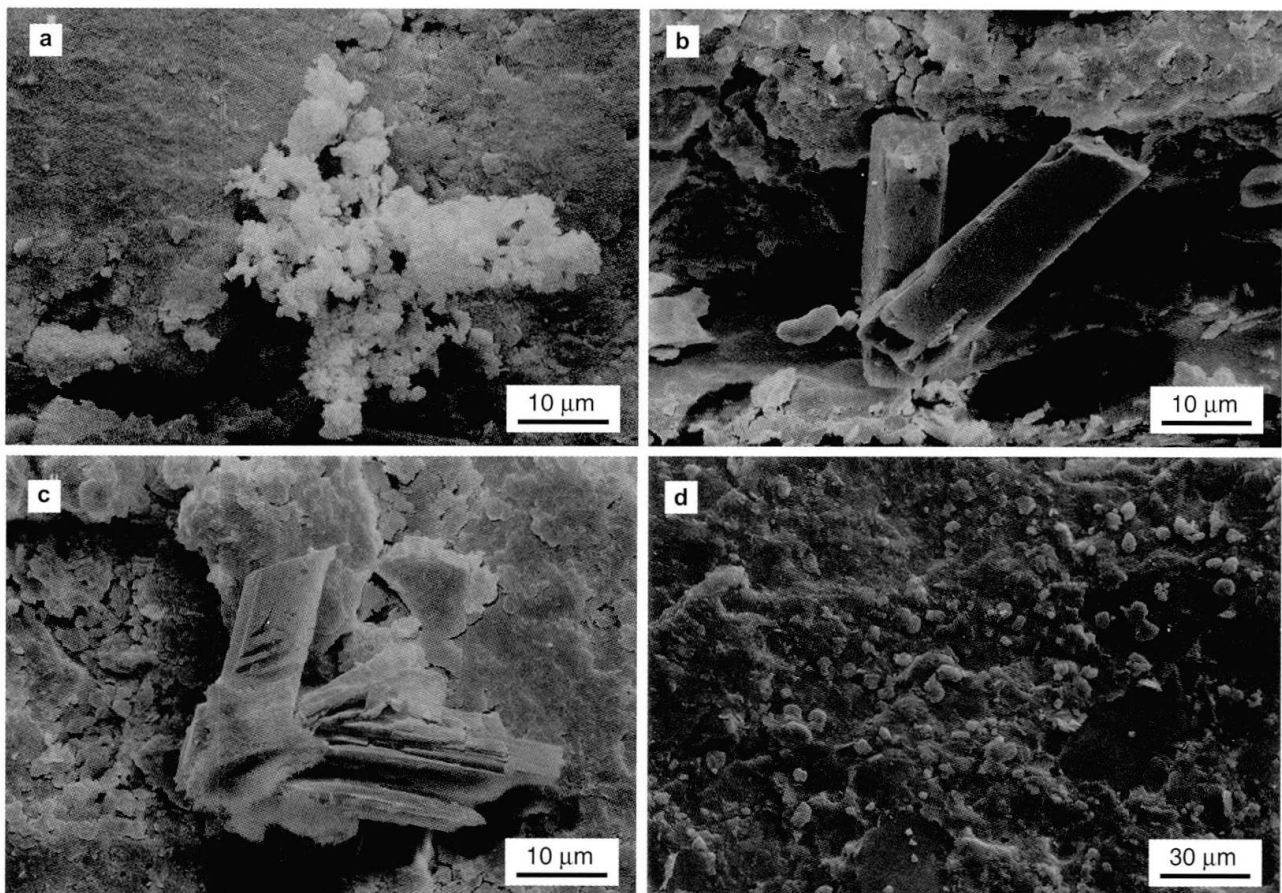

Fig. 3   SEM backscattered electron images of secondary minerals in the diffusion experiments. (a) C-A-S-H gel (after 4 months), (b) Ca zeolites (after 6 months), (c) Ca zeolite overgrown by C-(A-)S-H phase (after 6 months), (d) calcite precipitation zone (after 18 months).
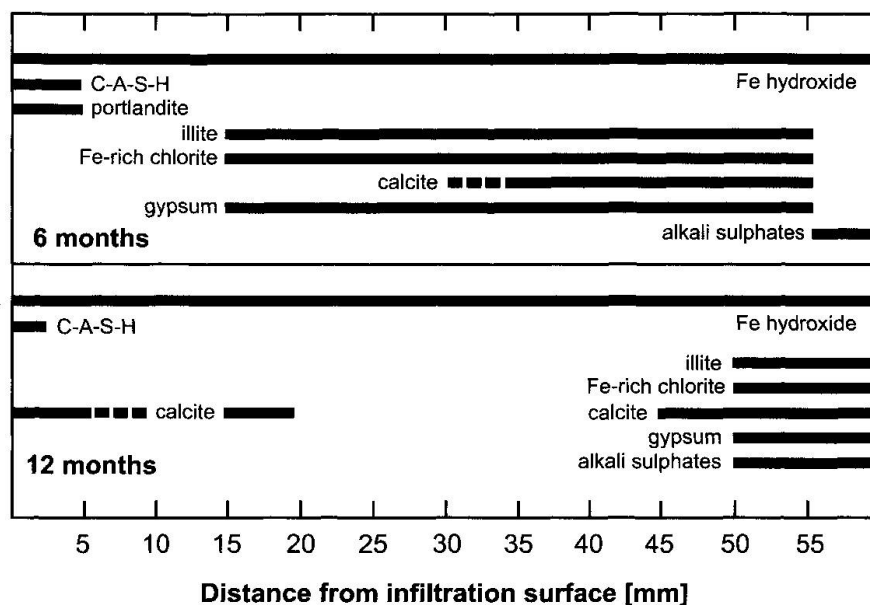
Fig. 4 Comparison of distribution of secondary minerals that formed in the advection experiments at different time steps. The right boundary of the graph represents the position of the evaporation surface of the rock sample. Dashed bars indicate uncertain identification of a mineral phase. See text for details. C-A-S-H: Ca–Al–Si-hydrate phase.

erally, secondary precipitates grew along discrete planar features of enhanced permeability such as bedding planes, interfaces of shell debris and micro-cracks.

After 7 months of reaction time, the zone adjacent to the infiltration surface is characterized by extensive formation of C-A-S-H phases, which exhibit fibrous morphology infilling micro-cracks in the rock matrix. XRD analyses indicate a poorly to non-crystalline phase. Small amounts of newly formed, perfectly idiomorphic portlandite (1–3 μm in diameter) is also present. The zone between 3 and 5 cm from the infiltration surface is characterized by an assemblage consisting of neoformed clay minerals, calcite and gypsum. According to XRD data, the clay mineral aggregates contain illite and chlorite (Fig. 5), and they can clearly be identified as neoformations as they exhibit a bright color in contrast to unaltered rock and characteristic fan-shaped morphologies (Fig. 6a). Quantitative chemical analyses by EDS yield illitic stoichiometry with highly variable contents of Fe and minor amounts of Mg indicating microscopic intergrowths of Fe-rich chlorite. The clay minerals show flaky morphology and grain sizes do not exceed 5 μm (Fig. 6b). Neoformed calcite occurs as tiny, finely dispersed crystals with a roundish shape. Gypsum forms lath-shaped crystals a few μm in length. The uppermost part of the profile adjacent to the evaporation surface is characterized by massive formation of alkali sulphates of syngenite (K–Ca) and glauberite (Na–Ca) composition.

After 12 months, the infiltration surface is completely covered by C-A-S-H phases with a foily appearance forming honeycomb structures (Fig. 6c) which are X-ray amorphous. The zone be-

tween 0 and 2 cm above the infiltration surface contains tiny, finely dispersed neoformed calcite crystals with roundish grain shapes. The zone beneath the evaporation surface hosts the most extensive mineral neoformations comprising calcite, clay minerals and sulphates in order of decreasing abundance. Calcite displays euhedral grain shapes and builds up dense covers on bedding planes
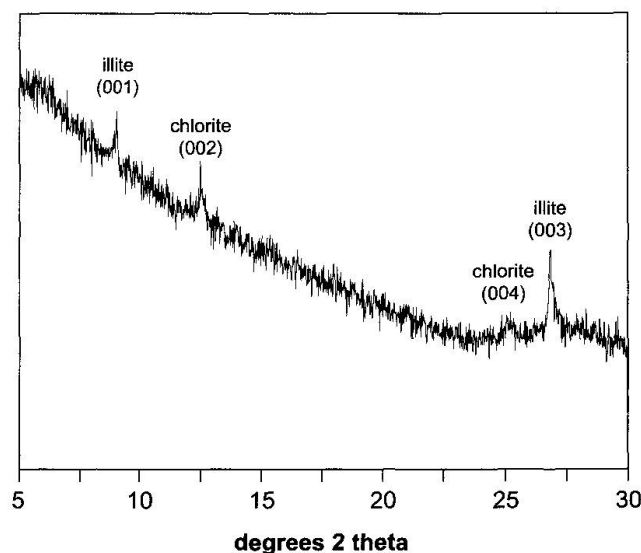
Fig. 5 X-ray diffraction pattern of neoformed clay mineral assemblages in the advection experiment after 7 months. The high background intensity towards low two theta angles is due to scattered X-rays as an effect of the long measurement durations which were essential for the identification of peaks on the very small amounts of reaction material available. The elevated intensity of the illite (003) diffraction peak with respect to the (001) peak is either due to quartz impurities or to imperfect orientation of the clay minerals parallel to the sample holder.

(Fig. 6d). Newly formed clay minerals exhibit flaky morphology with irregular grain shapes and were identified as the same illite-Fe-rich chlorite assemblages as found in the 7 month experiment based on equal chemical compositions and morphologies. Confirmation by XRD identification of these assemblages was not feasible due to insufficient amounts of reaction material.

The neoformed sulphates are gypsum and of syngenite composition (K–Ca). They form lath-shaped to fibrous crystals several μm in length.

Reaction products detected after 7 and 12

months are basically identical, whereas their position along the flow path differs (Fig. 4). An obvious feature is that the clay mineral-calcite-gypsum precipitation front propagates upwards with time towards the evaporation surface.

Discussion

The first minerals appearing in the diffusion experiments are C-A-S-H phases. Substitution of Al in C-S-H phases has been reported for tober-
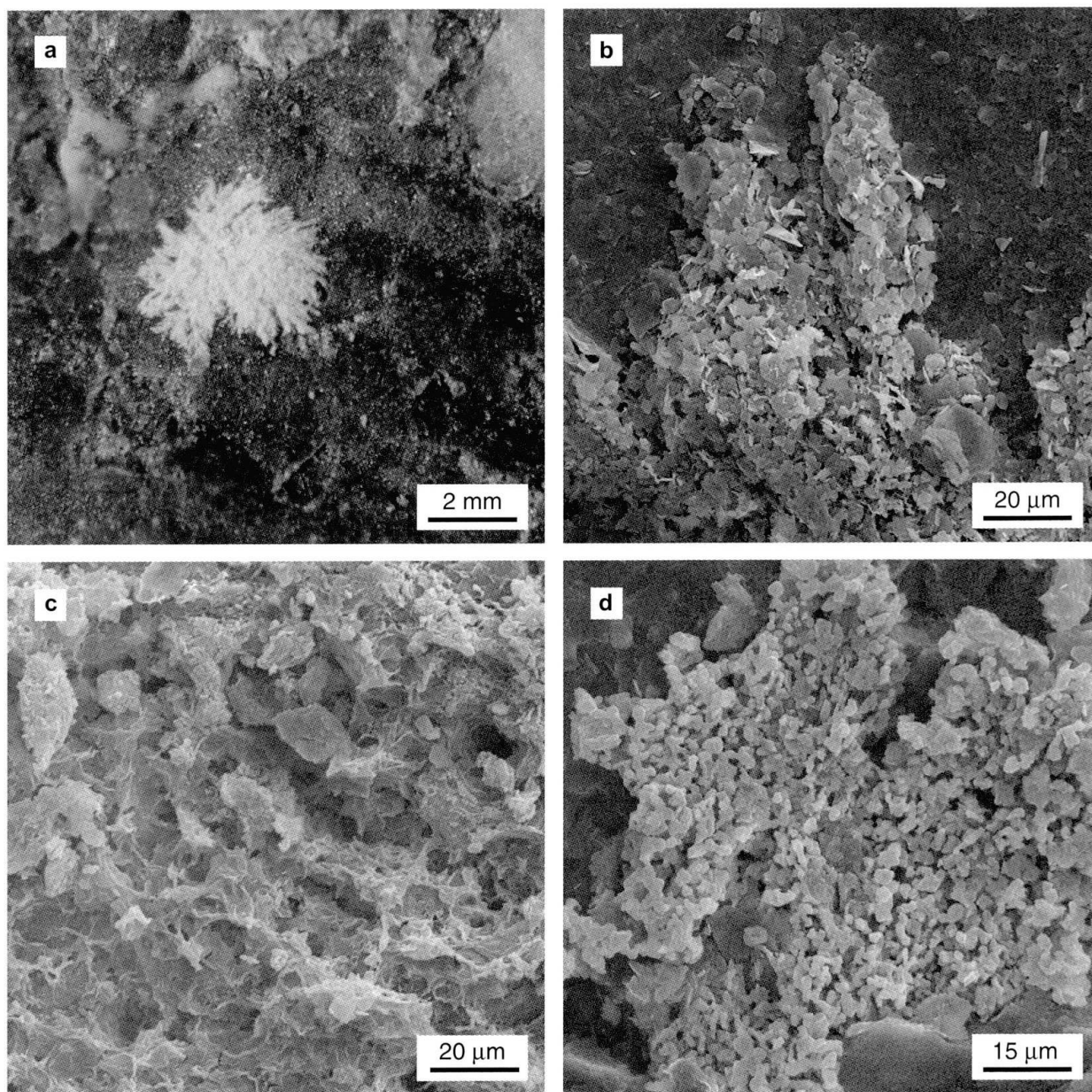
Fig. 6 Photographs of secondary minerals in the advection experiments. (a) binocular microscopic image of new clay mineral assemblage (white) on clay substrate (dark) (after 7 months), (b) SEM image of newly formed clay minerals (after 7 months), (c) SEM image of honeycomb textured C-A-S-H (after 12 months), (d) SEM image of massive calcite precipitation zone (after 12 months).

morite (MITSUDA and TAYLOR, 1978) and to a larger extent for tacharanite (CLIFF et al., 1975) where Al may be an essential constituent. The source of Al is kaolinite, which is readily attacked under highly alkaline conditions at temperatures as low as 30 °C (BAUER et al., 1998) and its consumption during reaction was confirmed by XRD. Dissolution of quartz was not directly observed, but its high reactivity at strongly alkaline conditions has been shown by CHERMAK (1992, 1993) and BATEMAN et al. (1997). Thus, the first important reaction in the diffusion experiments is likely to be:
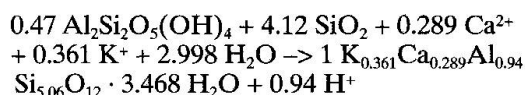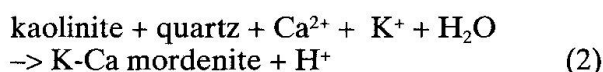
kaolinite + quartz + Ca^{2+} + H_2O
-> tacharanite + H^+ $\qquad$ (1)

1 $Al_2Si_2O_5(OH)_4$ + 16 SiO_2 + 12 Ca^{2+} +
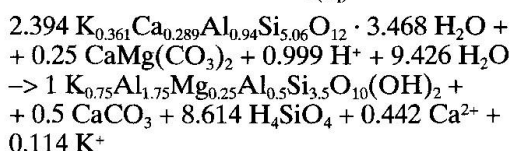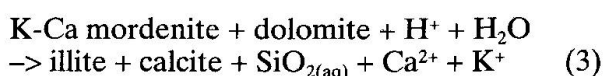28 H_2O -> 1 $Ca_{12}Al_2Si_{18}O_{51} \cdot$ 18 H_2O + 24 H^+
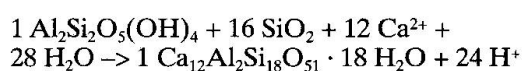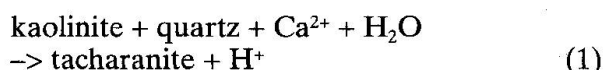
The hydrolysis of silicates and precipitation of C-A-S-H phases produce hydrogen ions resulting in a pH drop, as shown by the pH measurements on the reacted solutions. The decrease of pH results in the subsequent formation of zeolites of mordenite-dachiardite composition, which are indicative of pH values between 7 to 9 (MARINER and SURDAM, 1970; BARTH-WIRSCHING and HÖLLER, 1989) according to the reaction:

kaolinite + quartz + Ca^{2+} + K^+ + H_2O
-> K-Ca mordenite + H^+ $\qquad$ (2)

0.47 $Al_2Si_2O_5(OH)_4$ + 4.12 SiO_2 + 0.289 Ca^{2+}
+ 0.361 K^+ + 2.998 H_2O -> 1 $K_{0.361}Ca_{0.289}Al_{0.94}$
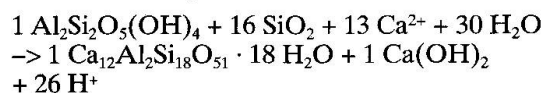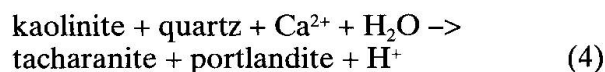$Si_{5.06}O_{12} \cdot$ 3.468 H_2O + 0.94 H^+

The observation of fibrous C-A-S-H phases overgrowing zeolites is most likely a consequence of periodic replacement of the high-pH solution. Infiltration of the new solution into the rock occurs along flow paths which have already reacted with high-pH fluid and this fluid will thus be less effectively buffered by the rock and overruns the zeolite precipitation zone at a stage where it is still high in pH precipitating C-A-S-H phases.
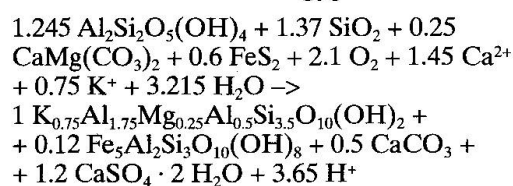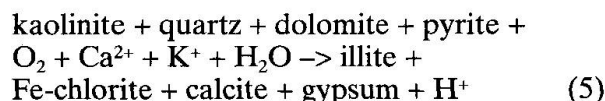
Early formed zeolite and C-A-S-H phases completely disappear after 12 months, and calcite forms presumably together with illite. Calcite precipitation is attributed to the dissolution of dolomite/ankerite, which will be discussed below. The appropriate reaction involving zeolite after 12 months is:

K-Ca mordenite + dolomite + H^+ + H_2O
-> illite + calcite + $SiO_{2(aq)}$ + Ca^{2+} + K^+ $\qquad$ (3)

2.394 $K_{0.361}Ca_{0.289}Al_{0.94}Si_{5.06}O_{12} \cdot$ 3.468 H_2O +
+ 0.25 $CaMg(CO_3)_2$ + 0.999 H^+ + 9.426 H_2O
-> 1 $K_{0.75}Al_{1.75}Mg_{0.25}Al_{0.5}Si_{3.5}O_{10}(OH)_2$ +
+ 0.5 $CaCO_3$ + 8.614 H_4SiO_4 + 0.442 Ca^{2+} +
0.114 K^+

Reaction products are more abundant in the advection than in the diffusion experiments as to be expected from higher mass transfers in the advection setup. Here, C-A-S-H phases and minor portlandite are forming on or near the infiltration surface according to:

kaolinite + quartz + Ca^{2+} + H_2O ->
tacharanite + portlandite + H^+ $\qquad$ (4)

1 $Al_2Si_2O_5(OH)_4$ + 16 SiO_2 + 13 Ca^{2+} + 30 H_2O
-> 1 $Ca_{12}Al_2Si_{18}O_{51} \cdot$ 18 H_2O + 1 $Ca(OH)_2$
+ 26 H^+

The presence of portlandite is a record of very low pCO_2 at the inlet zone. Again, the formation of the C-A-S-H phases causes a strong pH drop tending to neutralize the high-pH plume. C-A-S-H phases are therefore absent at greater distances from the inlet but followed by a clay mineral (illite and Fe-rich chlorite)-calcite-gypsum paragenesis according to:

kaolinite + quartz + dolomite + pyrite +
O_2 + Ca^{2+} + K^+ + H_2O -> illite +
Fe-chlorite + calcite + gypsum + H^+ $\qquad$ (5)

1.245 $Al_2Si_2O_5(OH)_4$ + 1.37 SiO_2 + 0.25
$CaMg(CO_3)_2$ + 0.6 FeS_2 + 2.1 O_2 + 1.45 Ca^{2+}
+ 0.75 K^+ + 3.215 H_2O ->
1 $K_{0.75}Al_{1.75}Mg_{0.25}Al_{0.5}Si_{3.5}O_{10}(OH)_2$ +
+ 0.12 $Fe_5Al_2Si_3O_{10}(OH)_8$ + 0.5 $CaCO_3$ +
+ 1.2 $CaSO_4 \cdot$ 2 H_2O + 3.65 H^+

It must be noted that pyrite oxidation is not bound to this particular stage but also occurs earlier, whereby most of the Fe is forming ferric iron hydroxides responsible for the rusty discoloration. The sulphate derived from pyrite oxidation is highly soluble in the solution such that saturation with respect to gypsum is attained at later stages.

In reaction 5, formation of calcite is controlled by the availability of CO_3^{2-} (dominant carbonate species at high pH) in solution rather than by Ca^{2+}, which is available in excess and buffered by concomitant gypsum precipitation. The lack of corrosion features on primary calcite suggests that the initial high-pH solution is close to saturation with respect to calcite. CO_3^{2-} is therefore produced by dissolution of dolomite/ankerite which is a very effective mechanism for calcite precipitation as two moles of CO_3^{2-} are released per mole dolomite/ankerite dissolved. Diffusion-reaction calculations by STEEFEL and LICHTNER (1998b) predict that the mechanism of CO_3^{2-} production by dolomite dissolution and interdiffusion with Ca^{2+} from the infiltrating high-pH solution has the potential to significantly reduce matrix porosity of a rock within tens to hundreds of years by massive calcite precipitation. The formation of calcite in

the present experiments occurs at the transition of a C-A-S-H/zeolite stage to a clay mineral-calcite stage in both experimental setups. Higher pCO_2 is therefore considered to be responsible for the disappearance of C-A-S-H and zeolite phases at posterior stages of rock-water reaction.

The same effect of CO_2 on mineral parageneses in low-grade metamorphic rocks (40–200 °C) has been found by ZEN (1974), who noted that a Ca zeolite trend at low fugacity of CO_2 can be distinguished from a clay mineral-carbonate trend for higher CO_2 fugacities. This is also demonstrated by equilibrium calculations in the system $CaO-Al_2O_3-SiO_2-CO_2-H_2O$ which limit the stability of zeolite assemblages to low pCO_2 (THOMPSON, 1971).

One of the main differences between the two experimental setups with regard to newly formed minerals is the lack of zeolites in the advection experiments. The formation of zeolites at low temperatures and highly alkaline conditions appears to be bound to closed systems, whereas open systems produce C-A-S-H phases. This is in agreement with previous studies on high-pH alteration of argillaceous rock: BATEMAN et al. (1999) produced C-A-S-H phases in open system column experiments but no zeolites, whereas CHERMAK (1992, 1993) grew various zeolite phases in closed system batch experiments although at much higher temperatures of 150 to 200 °C. As mentioned above, zeolites high in silica (as found in the present experiments) form in an environment of low pH between 7 to 9 (MARINER and SURDAM, 1970; BARTH-WIRSCHING and HÖLLER, 1989) and supersaturation with respect to silica (COOMBS et al., 1959). The low fluxes in the diffusion experiments allow for a greater extent of equilibration to decrease the pH locally and acquire enough Si and Al to precipitate zeolites compared to larger fluxes in open systems. Here, the high-pH fluid is less effectively buffered at the inlet zone so that C-A-S-H phases form. At greater distance from the inlet where zeolites would be stable with regard to silica saturation and pH, pCO_2 is too high, favouring precipitation of calcite and clay minerals.

Formation of illite, chlorite and calcite at the expense of kaolinite and dolomite/ankerite are reported from many low-grade metamorphic environments (ZEN, 1959; HUTCHEON, 1990; AHN et al., 1988) where lower pH and higher temperatures (100–200 °C) prevail. It is interesting to note that similar reactions occur in the present experiments (equation 5) although at much lower temperatures. Conditions of high pH thus seem to greatly increase reaction rates. Reaction calculations of the experimentally determined diffusion controlled mineral reactions indicate that these

reactions are controlled by kinetics rather than equilibrium, and that reaction rate constants for primary silicates (kaolinite, quartz) therefore play an important role. There appears to be a strong tendency to fast dissolution rates at highly alkaline conditions and low temperatures (ADLER et al., 1998). Experimental data on reaction rate constants for silicates under conditions of very high pH and low temperature are largely lacking.

The observation that most of the reaction products form on bedding planes or along clayshell debris interfaces emphasises the role of discrete planar features as major pathways for infiltrating solutions. The fact that fluid fluxes in the advection experiments remain quite constant throughout the experiments are a positive sign for the physical integrity of the rock samples. The relatively short duration of the experiments of up to 18 months is not sufficient to identify a long-term trend with regard to changes on the hydraulic conductivity of the rock due to mineral dissolution and precipitation reactions. As C-A-S-H phases and sulphates have large molar volumes compared to dissolving primary constituents, the reactions occurring during high-pH alteration of the rock are expected to decrease the porosity at least locally. Furthermore, STALDER (1973) stated that authigenic illite, due to its in-situ morphology, divides pore spaces into a large number of thin channels causing increased tortuosity and further reduces pore space because of water adsorption on the large available crystal surface area.

Several experimental observations afford a comparison to observations on naturally occurring hyperalkaline waters and associated rock alteration in Jordan. At the Maqarin site bordering the deeply incised Yarmouk River in Northern Jordan naturally occurring cement-like bodies are inferred to have formed from rehydrated pyrometamorphic combustion products of a bituminous biomicritic limestone. Subsequent percolation of groundwaters led to an hyperalkaline plume propagating along fracture-controlled flowpaths. Both, relatively evolved Ca–OH dominated flow systems are present and relatively younger alkali-rich systems. The younger K–Na-bearing systems are not completely exposed but do suggest a temporal sequence of mineralization initiated by a carbonate stage and followed by Ca–K–Na–Al zeolite-type, and several distinguishable C-S-H gel-type stages. Surficial seepages marked by portlandite-containing travertines, and dripping waters observed in reconnaissance galleries, reach pH values above 12. The Maqarin site is studied by an international working group motivated to examine long-term high-pH effects in the context of safe geologic disposal

of radioactive waste. Some general aspects were published by ALEXANDER (1995), ALEXANDER et al. (1995) and WABER and ALEXANDER (1995), and a large amount of details are provided by KHOURY and NASSIR (1982), ALEXANDER (1992), LINKLATER (1998) and SMELLIE (1999).

Both, the relative sequence of C-(A-)S-H and zeolite assemblages and its relation to open vs. closed system conditions is also inferred from observations at the Maqarin site, where the diffusion analogy would include processes in the rock matrix adjacent to advective features. Some high-pH water conducting features at Maqarin suggest a tendency to plug fracture apertures. Enhancement of pore space in the adjacent rock matrix through dissolution of silicates is observed in some cases. This features, also supported by the inferred rock-water reactions of this study, are specifically addressed by numerical modelling efforts of STEEFEL and LICHTNER (1998 a, b) for the situation at Maqarin. A principal difference between Opalinus Clay and the rocks at Maqarin are the low clay content (< 5%), the bituminous nature and the more prominent role of sulphur at the latter locality, leading also to the formation of ettringite in the alteration assemblages.

Conclusions

The aim of this experimental study was to determine the effect of high-pH K–Na–Ca-hydroxide solutions on Opalinus Clay under conditions relevant for the deep disposal of waste in a cementitious repository. The artificial high-pH solutions represent an early leachate expected from a cementitious repository and the experimental conditions simulate interactions that could occur in a repository environment where pore waters from the concrete interact with an argillaceous host rock. The experiments include two important innovations compared to previous studies, leading to more relevant results when applied to a repository situation. First, they relate to whole rock rather than crushed rock in order to more closely mimic host rocks, reactive surfaces and hydraulic regime and, second, they were conducted at low temperatures that are considered to match the conditions prevailing in potential cementitious repository systems. It has been demonstrated that mass transfer at low temperatures is traceable after short reaction times under a variety of conditions for the infiltration of a high-pH solution. The general sequence of reaction products includes, first, the precipitation of zeolites and/or C-A-S-H phases at the expense of kaolinite and quartz, followed by a clay mineral-calcite paragenesis. In-

creasing fugacity of CO_2 in the solution by dolomite/ankerite dissolution is responsible for the formation of partly massive calcite precipitation zones and is identified as key parameter for the disappearance of zeolite and C-A-S-H phases during later stages of rock-water interaction. The occurrence of zeolites is restricted to closed systems where conditions of low fluid fluxes allow for a greater degree of local pH buffering thus providing suitable conditions for zeolite precipitation at relatively low pH.

These experiments under high-pH conditions show similar reaction trends to those found in environments of higher temperatures and lower pH, indicating that the high-pH conditions greatly increase reaction rates. The results also assist in the interpretation of patterns observed in the natural analogue situation of hyperalkaline interaction at Maqarin.

References

ADLER, M., MÄDER, U. and WABER, H.N. (1998): Experiment vs. Modeling: Diffusive and advective interaction of high-pH solution in argillaceous rock at 30 °C. Mineralogical Magazine, 62A, 15–16.

AHN, J.H., PEACOR, D.R. and COOMBS, D.S. (1988): Formation mechanisms of illite, chlorite and mixed layer illite-chlorite in Triassic volcanogenic sediments from the Southland Syncline, New Zealand. Contrib. Mineral. and Petrol., 99, 82–89.

ALEXANDER, W.R. (Ed.) (1992): A natural analogue study of cement-buffered, hyperalkaline groundwaters and their interaction with a sedimentary host rock, Phase I: definition of source terms. Nagra Technical Report Series, NTB 91–10, Wettingen, Switzerland.

ALEXANDER, W.R. (1995): Natural cements: How can they help us safely dispose of radioactive waste? Radwaste Magazine 2, 5, Sept. 1995, 61–69.

ALEXANDER, W.R., MILODOWSKI, A.E., KHOURY, H.N. and SALAMEH, E. (1995): Why go to Jordan to worry about Wellenberg? A study of the interaction between cement derived hyperalkaline water and sedimentary rocks. Schweiz. Mineral. Petrogr. Mitt., 75, 467–468.

BARTH-WIRSCHING, U. and HÖLLER, H. (1989): Experimental studies on zeolite formation conditions. Eur. J. Mineral., 1, 489–506.

BATEMAN, K., COOMBS, P., NOY, D.J., PEARCE, J.M. and WETTON, P.D. (1997): Numerical modelling and column experiments to simulate the alkaline disturbed zone around a cementitious nuclear waste repository. 21st International Symposium on the Scientific Basis for Nuclear Waste Management, MRS'97, 313–314.

BATEMAN, K., COOMBS, P., PEARCE, J.M., NOY, D.J., ROCHELLE, C.A. and WETTON, P.D. (1999): Column Experiments Phase II. Unpublished Nagra Internal Report, Wettingen, Switzerland.

BAUER, A., VELDE, B. and BERGER, G. (1998): Kaolinite transformation in high molar KOH solutions. Applied Geochemistry, 13, 619–629.

BERNER, U. (1990): A thermodynamic description of the evolution of porewater chemistry and Uranium speciation during the degradation of cement. Nagra Technical Report Series, NTB, 90–12, Wettingen, Switzerland.

BROOKINS, D.G. (1987): Geochemical Aspects of Radioactive Waste Disposal. Springer Verlag, New York.

CHERMAK, J.A. (1992): Low temperature experimental investigation of the effect of high pH NaOH solutions on the Opalinus Shale, Switzerland. Clays and Clay Minerals, 40, 650–658.

CHERMAK, J.A. (1993): Low temperature experimental investigation of the effect of high pH KOH solutions on the Opalinus Shale, Switzerland. Clays and Clay Minerals, 41, 365–372.

CLIFF, G., GARD, J.A., LORIMER, G.W. and TAYLOR, H.F.W. (1975): Tacharanite. Mineralogical Magazine, 40, 113–126.

COOMBS, D.S., ELLIS, A.J., FYFE, W.S. and TAYLOR, A.M. (1959): The zeolite facies, with comments on the interpretation of hydrothermal syntheses. Geochim. Cosmochim. Acta, 17, 53–107.

DIAMOND, S., WHITE, J.L. and DOLCH, W.L. (1964): Transformation of clay minerals by calcium hydroxide attack. In: BRADLEY, W.F. (ed.): Clays and Clay Minerals. Proceedings of the twelfth national conference on clays and clay minerals. Pergamon Press, 359–379.

HAWORTH, A., SHARLAND, S.M., TASKER, P.W. and TWEED, C.J. (1987): Evolution of the groundwater chemistry around a nuclear waste repository. Scientific Basis for Nuclear Waste Management, XI, 425–434.

HUTCHEON, I. (1990): Clay-carbonate reactions in the Venture area, Scotian Shelf, Nova Scotia, Canada. In: SPENCER, R.J. and CHOU, I.M. (eds): Fluid-Mineral Interactions: A Tribute to H. P. Eugster. The Geochemical Society Special Publication, 2, 199–212.

KHOURY, H.N. and NASSIR, S. (1982): High temperature mineralisation in the Maqarin area, north Jordan. Neues Jahrb. Miner. Abh., 144, 197–213.

LINKLATER, C.M., ALBINSSON, Y., ALEXANDER, W.R., CASAS I., MCKINLEY, I.G. and SELLIN, P. (1996): A natural analogue of high-pH cement pore waters from the Maqarin area of northern Jordan: Comparison of predicted and observed trace-element chemistry of uranium and selenium. Journal of Contaminant Hydrology, 21, 59–69.

LINKLATER, C.M. (Ed.) (1998): A natural analogue study of cement-buffered, hyperalkaline groundwaters and their interaction with a repository host rock: Phase II. Nirex Science Report, S-98–003.

MARINER, R.H. and SURDAM, R.C. (1970): Alkalinity and formation of zeolites in saline alkaline lakes. Science, 170, 977–980.

MITSUDA, T. and TAYLOR, H.F.W. (1978): Normal and anomalous tobermorites. Mineralogical Magazine, 42, 229–235.

REARDON, E.J. (1990): An ion interaction model for the determination of chemical equilibria in cement/water systems. Cement and Concrete Research, 20, 175–192.

SMELLIE, J.A.T., KARLSSON, F. and ALEXANDER, W.R. (1997): Natural analogue studies: present status and assessment implications. Journal of Contaminant Hydrology, 26, 3–17.

SMELLIE, J.A.T. (Ed.) (1999): Maqarin natural analogue study: Phase III. SKB Technical Report, TR-98-04, volume I and II.

STALDER, P.J. (1973): Influence of crystallographic habit and aggregate structure of authigenic clay minerals on sandstone permeability. Geologie en Mijnbouw, 52, 217–220.

STEEFEL, C. I. and LICHTNER, P.C. (1994): Diffusion and reaction in rock matrix bordering a hyperalkaline fluid-filled fracture. Geochim. Cosmochim. Acta, 58, 3595–3612.

STEEFEL, C. I. and LICHTNER, P.C. (1998a): Multicomponent reactive transport in discrete fractures I: Controls on reaction front geometry. J. Hydrol., 209, 186–199.

STEEFEL, C. I. and LICHTNER, P.C. (1998b): Multicomponent reactive transport in discrete fractures II: Infiltration of hyperalkaline groundwater at Maqarin, Jordan, a natural analogue site. J. Hydrol., 209, 200–224.

THOMPSON, A.B. (1971): P CO_2 in Low-Grade Metamorphism; Zeolite, Carbonate, Clay Mineral, Prehnite Relations in the System $CaO-Al_2O_3-SiO_2-CO_2-H_2O$. Contrib. Mineral. and Petrol., 33, 145–161.

WABER, H.N. and ALEXANDER, W.R. (1995): Von natürlichem Zement bis zum Endlager Beton. Schweiz. Techn. Zeitschrift 12/95, STV-Verlags AG, Zürich, Switzerland.

ZEN, E.-A. (1959): Clay mineral-carbonate relations in sedimentary rocks. Amer. J. Sci., 257, 29–43.

ZEN, E.-A. (1974): Burial Metamorphism. Canadian Mineralogist, 12, 445–455.